

The collecting effect of *Rhodotorula rubra* on cassiterite and co-existing minerals

Lihong Lan¹, Shujuan Jin¹, Yiwen Wu¹, Qiaoqiong Huang², Yuxian Feng³, Zhuo Yang¹, Ping Lan¹, Heping Li¹, Bo Peng¹

¹ Guangxi Key Laboratory for Polysaccharide Materials and Modifications, Guangxi Minzu University, Nanning 530006, PR China

² Laibin China Tin Smelting Co., Ltd, 546102.

³ Institute of New Functional Materials, Guangxi Institute of Industrial Technology, Nanning 530022, PR China.

Corresponding author: lanlihong2004@163.com (Lihong Lan)

Abstract: This study investigated the novel application of *Rhodotorula rubra* as a bio-based collector for selective flotation separation of cassiterite from co-existing minerals, quartz and calcite. Under optimal conditions (*Rhodotorula rubra* suspension concentration: 2.0g/L, pH=5, and sodium silicate dosage: 3.75 g/L), a cassiterite recovery rate of 65% was achieved, demonstrating effective mineral selectivity. Fourier-transform infrared spectroscopy analysis revealed that the adhesion mechanism between *Rhodotorula rubra* and cassiterite involved synergistic physical adsorption and chemisorption interactions. These findings provide critical insights into the potential of microbial-based flotation agents for sustainable mineral processing.

Keywords: cassiterite, *Rhodotorula rubra*, biological collector, flotation separation

1. Introduction

Tin resources, as a critical rare metal in modern industry, play indispensable roles across multiple sectors including electronics, renewable energy, aerospace, and alloy manufacturing (Yu et al., 2021). These applications leverage tin's unique combination of advantageous properties, particularly its ductility, chemical stability, corrosion resistance (Li et al., 2023), low melting point, and non-toxic characteristics (Miao et al., 2024). Despite China's status as the holder of the world's largest tin reserves (Qiu and Huang, 2016) persistent challenges remain in optimizing resource utilization efficiency, primarily due to technical limitations in fine-grained cassiterite recovery processes.

Cassiterite beneficiation predominantly employs gravity separation and flotation methods, selected based on the mineral's particle size, density, and crystal structure (Angadi et al., 2015; Fu et al., 2024). However, the brittle nature of cassiterite causes excessive fragmentation during grinding processes. Conventional gravity separation techniques produce slimes when processing fine-grained cassiterite, leading to suboptimal recovery rates (Zhang et al., 2020). To mitigate this limitation, flotation has emerged as a critical method for separating fine and ultra-fine cassiterite particles, significantly improving resource utilization efficiency.

The separation of cassiterite is complicated by its association with common gangue minerals such as quartz, fluorite, calcite, hematite, sulfides, and tourmaline (Zhu et al., 2020). While recovering fine cassiterite from tailings represents a critical industrial priority (Zhang, 2010), existing flotation methods face challenges in achieving cost-effective selectivity. Current research emphasizes the development of efficient collector molecules, but their limited applicability to fine-grained ores remains a major obstacle to optimizing recovery rates (Chen, 2014; Liu et al., 2014; Qiu et al., 2018).

Traditional cassiterite flotation collectors encompass butyl xanthate, ethyl xanthate (Guo et al., 2016), carboxylic acids (Yin and Wang, 2014), CS-6 (a pink-to-orange paste with a pronounced fatty odor) (Cao et al., 2022), ZK-9 (a lighter pink paste with milder odor) (Yu et al., 2013), TM agents (Yang et al., 2012; Shang, 2015), and combined reagents like BK411/BK412 (Balasubramanian et al., 2012) and YK-SN/SN-

705 (Vasanthakumar et al., 2014). While CS-6 demonstrates superior collecting capacity over ZK-9, its practical application is constrained by poor selectivity. Conversely, ZK-9 exhibits limited efficacy in fine cassiterite flotation and faces cost-related implementation barriers. Anionic collectors, including fatty acids, arsine acids, and hydroxamic acids, have also been extensively utilized (Zheng et al., 2021; Chang et al., 2023). Fatty acids, despite their environmental compatibility and low dosage requirements, suffer from non-selective adsorption across multiple mineral surfaces, significantly compromising tin recovery efficiency (Peng et al., 2019). Although arsine acids were historically favored for their strong collecting ability, their high toxicity and environmental risks have led to widespread phase-out (Wang, 2013). Hydroxamic acids provide effective chelation with reduced toxicity but encounter industrial scalability challenges due to intricate synthesis protocols and elevated production costs (Chen et al., 2021).

Conventional gravity separation methods often fail to achieve satisfactory recovery rates for fine cassiterite particles, leading to substantial losses exceeding 80% of national tin reserves from processed ores (Lan et al., 2015). This inefficiency is exacerbated by rapid resource depletion driven by escalating domestic demand (Su et al., 2017). In contrast to chemical-based flotation, microbial flotation has emerged as a sustainable alternative for recovering low-grade and fine-grained cassiterite from tailings (Sreenivas and Padmanabhan, 2002; Wang, 2015). Research demonstrates that microorganisms such as *Bacillus* species, yeast fungi (Yuan et al., 2000; Yuan et al., 2000), and *Thiobacillus ferrooxidans* (Yu, 2013; Li et al., 2016; Korneli et al., 2013) function as bio-agents to enhance mineral recovery through selective surface property modification (Sarvamangala and Natarajan, 2009; Hemalatha and Kannan, 2011). Despite its potential, microbial flotation remains underexplored in fine cassiterite processing, with limited literature specifically addressing its technical feasibility.

2. Materials and methods

2.1. Materials

The microorganism species *Rhodotorula rubra* used in this study was purchased from the China General Microorganism Culture Collection Center. Cassiterite employed in the experiment had a purity of 99% and a particle size of 74~38 microns, sourced from Nandan Dachang, Guangxi. Both quartz and calcite were obtained from Sinopharm Chemical Reagent Co, Ltd, with purities of 99% and particle sizes of 74~38 microns. Based on the XRD analysis results (Fig. 1), the ore sample exhibited distinct high- and low-impurity mineral phases, enabling its use in pure-mineral flotation tests.

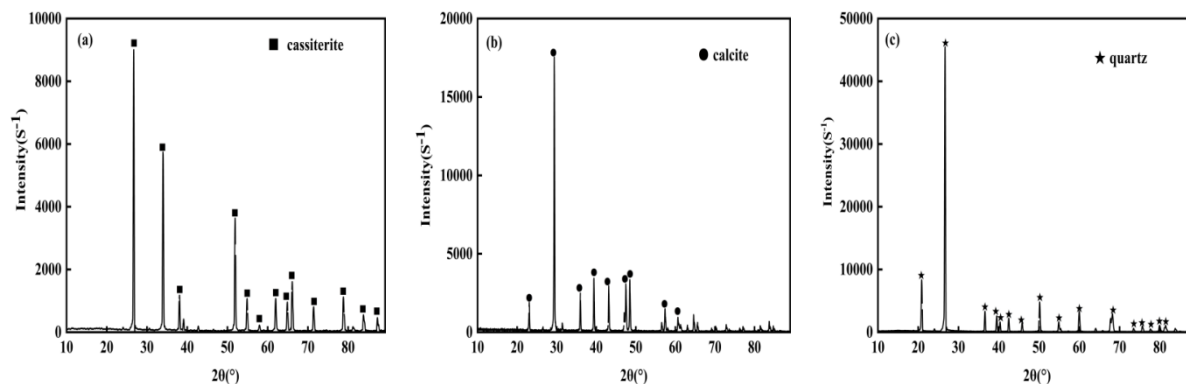


Fig. 1. (a) XRD patterns of cassiterite; (b) XRD patterns of calcite; (c) XRD patterns of quartz.

2.2. Preparation of microbial suspension

Culture media were prepared with the following composition per liter: 20 g glucose, 5 g peptone, and 5 g yeast extract, adjusted to pH 5.0. Aliquots of 200 mL media were placed in 500 mL glass flasks and sterilized by autoclaving at 121 °C for 30 minutes. After cooling to room temperature, a 24-hour pre-culture of *Rhodotorula rubra* ($OD_{600} \approx 1.0$) was aseptically inoculated at 2% (v/v), corresponding to 4 mL of inoculum per 200 mL medium. The inoculated flasks were transferred to a mechanical shaking table at 28 °C and shaken for 72 hours at 150 r/min. The microbial suspension was centrifuged at 1000 r/min

for 5 minutes. The supernatant was then re-centrifuged at 10,000 r/min for 15 minutes to obtain wet fungi sludge. The sludge was diluted with distilled water and re-centrifuged. This dilution-centrifugation process was repeated three times. Each dilution was followed by centrifugation at 10,000 r/min for 15 minutes. The wet weight of the sludge was measured. Finally, 0.5% NaCl was added to the fungal sludge to prepare working microbial suspensions of varying concentrations, which were stored at 4 °C (Yang et al., 2016; Jia et al., 2011; GB/T 10574.1 - 2003).

2.3. Recovery rates measurement

Using a mechanical stirrer (impeller diameter: 10 mm), a mineral sample (4.0 g) was placed in a 80 mL flotation cell, and the working microbial suspension was added under continuous shaking to ensure dispersion. The pH of the pulp was adjusted to the desired value using NaOH and HCl solutions. The pulp was thoroughly stirred, aerated, and subjected to flotation; froth products were scraped for 5 minutes. Both the collected foam and the remaining products at the bottom of the flotation cell were filtered, dried, and weighed to determine recovery rates. Each experimental group was tested in triplicate, and the average value was calculated. The recovery rate was calculated using the following formula (Merma et al., 2013; Jiang et al., 2007).

$$\text{Recovery rates} = \left[\frac{M_{\text{concentrate}}}{(M_{\text{concentrate}} + M_{\text{tailing}})} \right] \times 100 \quad (1)$$

where $M_{\text{concentrate}}$ is the mass of the concentrate (g), M_{tailing} is the mass of the tailing (g).

2.4. Measurement of surface potentials of minerals

A total of 4.0 g of ore sample was dispersed with distilled water to prepare a 50 g/L pulp. The pH value was adjusted to the desired level using sodium hydroxide and hydrochloric acid solutions. The pulp was injected into the sample tank using a syringe. Surface potential of each pure mineral was measured at specified pH values using a Malvern Surface Potentiometer. Average values were obtained after repeating the process through 7 measurement cycles (Chen., 2009).

A total of 1.0 g of ore sample was added to a beaker containing 50 mL of a known microbial suspension and stirred for 15 minutes in a magnetic stirrer at 400 r/min. The stirred pulp was left to rest for 15 min, after which the supernatant was poured out. Finally, the solid precipitate was dried in an oven at 80 °C for 12 h and subsequently analyzed by IR spectroscopy using the potassium bromide pellet method.

3. Results and discussion

3.1. Effect of the concentration of *Rhodotorula rubra* on the floatability of cassiterite

By changing the concentration of *Rhodotorula rubra* under the steady conditions of pulp concentrations of 50 g/L, pH = 5, temperature at 25 °C, and blending revolution of 2500 r/min, the effect of the concentration of *Rhodotorula rubra* on cassiterite recovery could be obtained, as shown in Fig. 2. With the increase in *Rhodotorula rubra* concentration, the recovery rate of cassiterite increased. When the concentration of the microbial suspension was 2.0 g/L, the recovery of cassiterite reached 74.24%. The saturation of the microbial adsorption on the mineral surface may have resulted in the recovery rate of cassiterite not improving further following the increase in microbial suspension to 2.0 g/L.

3.2. Effect of the pH value on the floatability of pure minerals

Under the conditions of the fungi solution concentration of 2.0 g/L, a temperature of 25 °C, pH = 5, and blending theory revolution of 2500 r/min, the pH value of the pulp during the flotation process was altered to explore the influence of the pH value on the floatability of cassiterite, quartz, and calcite. The results are presented in Fig. 3.

At 2.0 g/L *Rhodotorula rubra*, 25 °C, and 2500 r/min, pH adjustments altered floatability of cassiterite, quartz, and calcite (Fig. 3). Cassiterite recovery maximized (~70%) at pH = 5. Quartz recovery remained <15% due to innate non-floatability. Calcite recovery increased with *Rhodotorula rubra* but was pH-

insensitive, indicating *Rhodotorula rubra* acts as a weak calcite collector. Thus, calcite suppression is essential for tin ore separation.

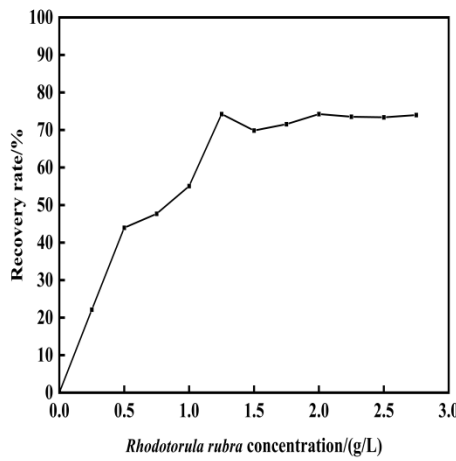


Fig. 2. Effect of *Rhodotorula rubra* concentration on cassiterite recovery

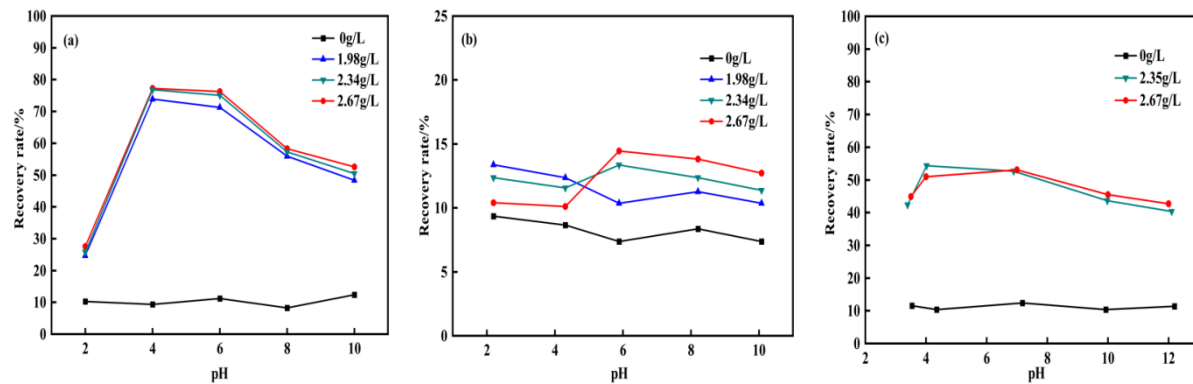


Fig. 3. (a) Effect of pH on cassiterite recovery; (b) effect of pH on quartz recovery; (c) effect of pH on calcite recovery

3.3. Selection of inhibitors

Starch, oxalic acid, and sodium silicate were selected as the inhibitors used to conduct the flotation process of the purified minerals. The experiment's results are presented in Fig. 4.

As Fig. 4 (a) exhibits, with the increase in the starch dosage, the recovery rates of cassiterite and quartz gradually decreased, but the recovery rate of calcite presented an upward trend. As can be observed in Fig. 4 (b), when oxalic acid was used as an inhibitor, the recovery rate of cassiterite slightly decreased with the added dosage of oxalic acid. The floatability of quartz was poor and the inhibition effect of oxalic acid was not obvious. The recovery rate of calcite fluctuated at approximately 70%. It was determined that oxalic acid had a poor inhibition effect on the calcite. Fig. 4 (c) shows that when sodium silicate is used as an inhibitor, the recovery rate of calcite decreases with the increase in sodium silicate concentration from the initial 50% to 25%. The recovery rate of cassiterite decreased with the increase in sodium silicate concentration; however, the rate was always higher than 60%. The recovery rate of quartz was stable at approximately 15%. When the concentration of sodium silicate was 3.75 g/L, the recovery rate of cassiterite was 65%. This selective depression aligns with polysaccharide depressants (e.g., *Tamarindus indica* kernel gum) in phosphate flotation systems: both preferentially adsorb on calcite rather than target minerals (e.g., fluorapatite/cassiterite). Critically, their adsorption mechanisms differ fundamentally: Polysaccharides chemically bind to Ca-sites via deprotonated hydroxyl groups (Yang et al., 2025). Sodium silicate forms colloidal silicic acid layers that physically shield calcite surfaces from collector attachment.

Therefore, sodium silicate can be used as an effective inhibitor of calcite in the microbial flotation of tin ore.

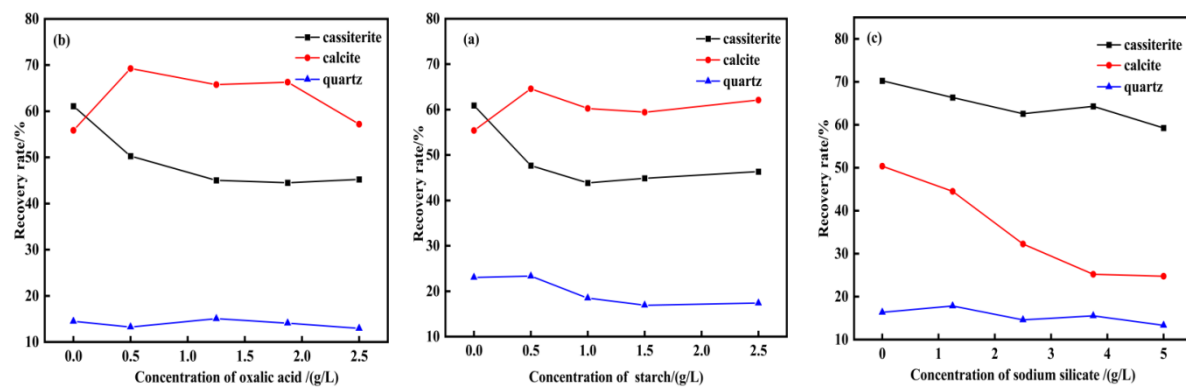


Fig. 4. (a) Effect of starch dosage on recovery of three minerals; (b) effect of oxalic acid dosage on recovery of three minerals; (c) effect of sodium silicate dosage on recovery of three minerals

3.4. Effect of the inhibitor on *Rhodotorula rubra*

To assess sodium silicate (Na_2SiO_3) effects on *Rhodotorula rubra* activity and flotation stability, sterilized base medium (20 g/L glucose, 5 g/L peptone, 5 g/L yeast extract, 15 g/L agar; pH 5.0 pre-sterilization) was supplemented aseptically with Na_2SiO_3 at final concentrations of 0 (control), 0.5, 2.5, and 5.0 g/L during cooling (45–50 °C). The medium was poured into Petri dishes, spot-inoculated with 1 mL of 36-h logarithmic-phase *Rhodotorula rubra* culture, and incubated at 30 °C for 36 h. Growth results are shown in Fig. 5.

By observing the culture results presented in Fig. 5, it is evident that although the color of the medium deepens with increasing sodium silicate concentration, the growth of *Rhodotorula rubra* remains robust across all concentrations tested (0–5.0 g/L). No visible inhibition of growth was observed, indicating that sodium silicate does not adversely affect the activity of *Rhodotorula rubra* under these conditions.

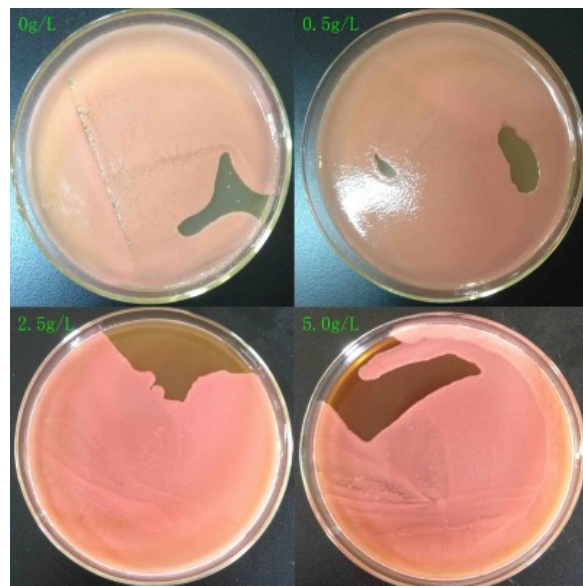


Fig. 5. Influence of sodium silicate concentration on *Rhodotorula rubra* growth

3.5. Surface potential analysis

When microorganisms adsorb on mineral surfaces, they alter surface physicochemical properties, activating, flocculating, or dispersing minerals. Surface potential changes are thus key to evaluating bio-collector efficacy. Hence, surface potentials of *Rhodotorula rubra*, cassiterite, quartz, and calcite were measured (Fig. 6).

As shown in Fig. 6a, *Rhodotorula rubra* exhibits an isoelectric point (IEP) at pH 1.4, bearing a negative charge above this pH. Its cell surface contains extracellular proteins, lipids, and polysaccharides, whose

charge properties govern fungal surface behavior across pH ranges. Extracellular proteins are amphoteric; they become negatively charged when solution pH exceeds their individual IEPs.

Cassiterite (IEP pH 4.3) is positively charged below pH 4.3. Within pH 1.4–4.3, opposite charges between cassiterite (+) and *Rhodotorula rubra* (−) enable electrostatic attraction—the key mechanism driving fungal adsorption onto cassiterite. Maximal cassiterite potential change at pH 5 aligns with optimal fungal activity.

Fig. 6b shows quartz IEP at pH 1.3. At flotation pH 5, both quartz and cassiterite are negatively charged, inducing electrostatic repulsion that prevents *Rhodotorula rubra* adsorption. For calcite (IEP pH 5.0), zero surface charge at pH 5 eliminates electrostatic interactions (Fig. 6c). However, significant post-adsorption potential changes on calcite confirm non-electrostatic mechanisms. The observed surface potential changes directly correlate with flotation selectivity, as evidenced by preferential *Rhodotorula rubra* adsorption on cassiterite over quartz/calcite. Such mechanisms mirror synergistic co-adsorption in conventional flotation, where combined collectors (e.g., NaOL/CTAC) separate minerals with similar charges via interfacial activity rather than electrostatics (Gong et al., 2025).

Rhodotorula rubra not only caused minerals to float through the electrostatic attraction, but also changed their surface potentials, so as to change their surface wettability properties and cause them to float, analogous to nanobubble effects enhancing cassiterite recovery (Ren et al., 2023). This wettability modification fundamentally alters mineral surface potential, enabling bubble attachment. Additionally, fungal cell-surface components (e.g., hydrophobic protein domains) mediate adsorption via chemical/hydrophobic interactions, particularly critical for calcite where electrostatic forces are absent.

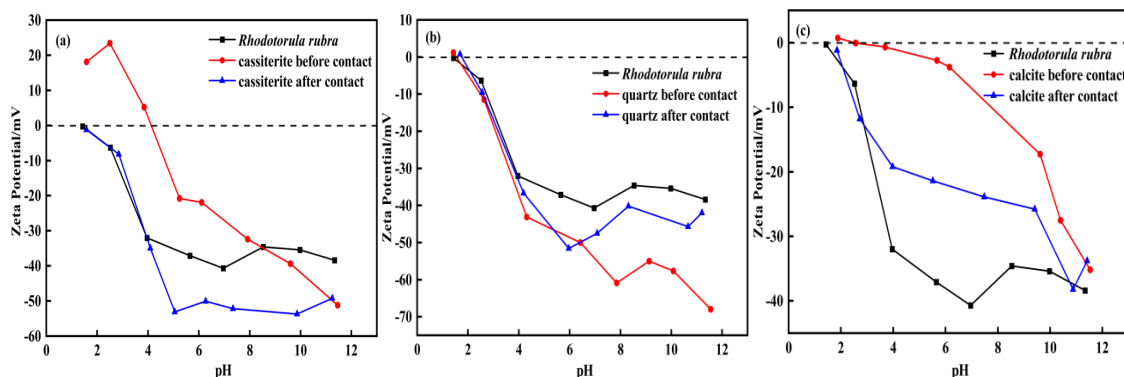


Fig. 6. (a) Surface potential changes before and after cassiterite is treated with *Rhodotorula rubra*. (b) Surface potential changes in quartz before and after the interaction with *Rhodotorula rubra*. (c) Surface potential changes in calcite before and after interaction with *Rhodotorula rubra*

3.6. Flotation of artificial mixed ore

The refined tin ore and quartz with an initial grade of 59.28% were mixed at the mass ratios of 1:9, 2:8, 3:7, 4:6, 5:5, and 6:4, respectively. Then, the flotation process was performed under the conditions of a fungi solution concentration of 3.33 g/L, sodium silicate concentration of 1.67 g/L, slurry concentration of 50 g/L, and pH = 5. The results are presented in Table 1. It can be observed in Table 1 that the recovery rate of the concentration increases with the increase in the mixed grade following a rough separation of the mixed ore. With the increase in the specific gravity of tin ore in the mixture, the recovery of tin ore and the grade of Sn in the concentrate improved.

Table 1. Flotation of mixed ore by *Rhodotorula rubra*

M _{tin} : M _{quartz}	Recovery rate / %	The grade of the Sn / %
1:9	29.50	8.79
2:8	33.94	46.69
3:7	43.74	39.10
4:6	51.68	42.20
5:5	59.07	49.62
6:4	62.34	56.88

3.7. Analysis of surface tension

Surface tension is an important factor to determine whether a substance has surface activity. In the experiment, it was observed that bubbles were easily generated in *Rhodotorula rubra* suspension; therefore, the surface tension of the suspension with different concentrations of the fungi and the pH value of the solution at maximum surface activity were measured. The results are presented in Fig. 6 - 7.

At pH = 5 and temperature of 23 °C, the surface tension of *Rhodotorula rubra* suspensions with different concentrations was measured. As can be observed in Fig. 7, the surface tension of the microbial suspension decreases with the increase in the concentration. When the fungi concentration of the solution increased to 1.5 g/L, the surface tension did not decrease, and the surface activity of the fungi solution was at its greatest. When the concentration of the fungi solution was 2.0 g/L and the temperature was 23 °C, the pH value of the fungi solution was changed to determine the influence of the pH value on the surface tension of the fungi solution.

The result is presented in Fig. 8. With the increase in the pH value, the surface tension of the microbial suspension first decreases and then increases, and has a minimum value of 48 mN/m when the pH is 7. The results show that *Rhodotorula rubra* suspension presents a certain surface activity when the fungi concentration is 2.0 g/L and pH is 5. This reduced interfacial tension enhances fungal adsorption capacity by improving cell-mineral contact efficiency, analogous to the synergistic effect of combined collectors (e.g., NaOL/CTAC) in conventional flotation systems where lowered surface tension correlates with enhanced mineral-collector interactions (Gong et al., 2025). These surface activity characteristics (especially at pH 5) directly enhance the adsorption capacity of *Rhodotorula rubra* on mineral surfaces, which correlates with the subsequent FTIR evidence of interfacial bonding mechanisms.

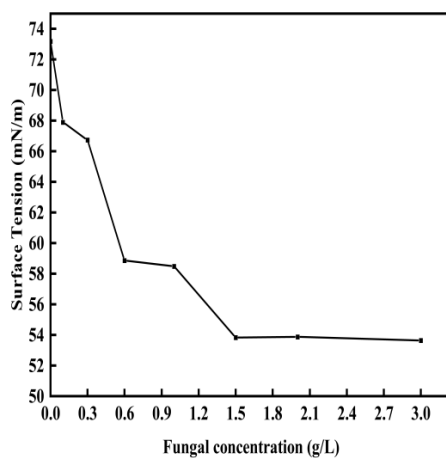


Fig. 7. Effect of the fungi solution concentration on surface tension

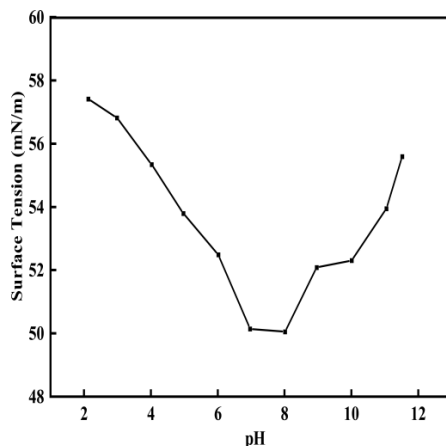


Fig. 8. Influence of pH on surface tension

3.8. Infrared spectral analysis

The IR spectra of *Rhodotorula rubra* before and after the interaction with cassiterite and quartz are presented in Fig. 9 - 11.

It can be observed from Fig. 9 that *Rhodotorula rubra* has a relatively wide absorption peak close to 3381.83 cm⁻¹, which is the stretching vibration absorption peak of intermolecular hydrogen bonds O-H and N-H. There are two small peaks close to 2924.86 cm⁻¹ and 2854.17 cm⁻¹, which should be the absorption peaks of the C-H stretching vibration of alkanes. The absorption peak close to 1745.19 cm⁻¹ is the C=O stretching characteristic of the aldehyde. The absorption peak close to 1653.62 cm⁻¹ is the C=O stretching vibration absorption peak of amide. The absorption peaks close to 1545.40 cm⁻¹ are the C-N stretching vibration absorption and N-H deformation vibration, which are equivalent to the shear vibration mode of -CH₂. The absorption peaks close to 1457.75 cm⁻¹ are -CH₃ antisymmetric deformation and -CH₂ vibration deformation. The absorption peak close to 1378.50 cm⁻¹ is the C-H bending vibration peak of alkanes. The absorption peak close to 1242.46 cm⁻¹ is the intermolecular C=O stretching vibration peak. The absorption peak close to 1071.61 cm⁻¹ is the stretching vibration peak of ether and the vibration peak of aliphatic ether.

As can be observed from Fig. 10, a new absorption peak appears following the interaction of cassiterite and *Rhodotorula rubra*, which is at 3381.83 cm⁻¹ and results from the stretching vibration absorption peak of intermolecular hydrogen bonds O-H and N-H. The absorption peak at 1640.60 cm⁻¹ was the C=O stretching vibration absorption peak of amide on the surface of *Rhodotorula rubra* cells. The C=O stretching vibration absorption peak of amide is observed at 1640.60 cm⁻¹, indicating a shift from its original position at 1653.62 cm⁻¹. This shift suggests that the carbonyl groups (C=O) of amides on *Rhodotorula rubra* are involved in interactions with cassiterite surface. Specifically, these C=O groups could form hydrogen bonds or coordination bonds with Sn-O sites on cassiterite surface. An obvious new absorption peak appears at 1118.87 cm⁻¹, which is the stretching vibration peak of ether aliphatic ether on the surface of *Rhodotorula rubra*. This indicates that *Rhodotorula rubra* can adsorb cassiterite well, and the adsorption force between *Rhodotorula rubra* and cassiterite is the common result of physical and chemical adsorption.

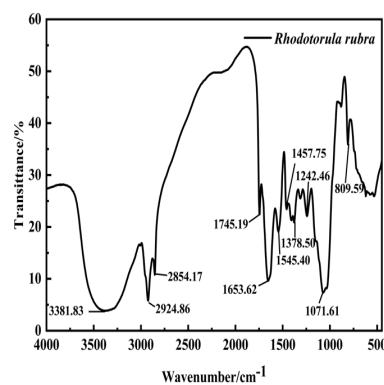


Fig. 9. IR spectra of *Rhodotorula rubra*

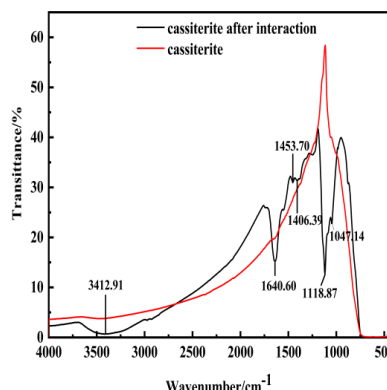


Fig. 10. IR spectra of cassiterite before and after the interaction with *Rhodotorula rubra*

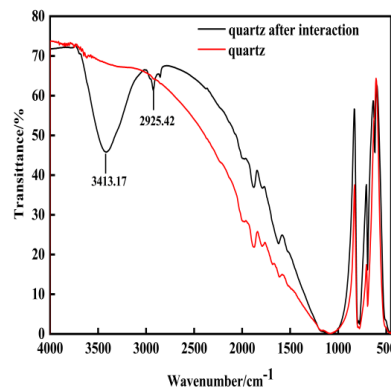


Fig. 11. Infrared spectrum of quartz treated with *Rhodotorula rubra*

4. Conclusions

In this study, *Rhodotorula rubra* was successfully employed as a bio-collector for the flotation separation of cassiterite from co-existing quartz and calcite. Through systematic optimization of the fungi concentration (2.0 g/L), sodium silicate dosage (3.75 g/L), and pulp pH (5.0), a maximum cassiterite recovery of 65% was achieved while effectively suppressing quartz and calcite flotation. Key mechanistic insights revealed that:

Selective electrostatic attraction between negatively charged *Rhodotorula rubra* and positively charged cassiterite (pH 1.4–4.3) drove preferential adsorption, while charge repulsion inhibited attachment to quartz at pH 5. Non-electrochemical mechanisms (hydrogen bonding/coordination via C=O groups; wettability modification) enabled calcite interaction despite zero surface charge at IEP. Intrinsic surfactant properties minimized pulp surface tension (48 mN/m at pH 7). Critically, *Rhodotorula rubra* offers significant sustainability advantages: low toxicity, biodegradability, alignment with Green Mineral Processing principles, reduced reliance on conventional chemical reagents, and carbon neutrality potential through cultivation on renewable biomass.

For industrial implementation, future work should address: Stability in complex pulp systems with multi-ion interference Cost-effective large-scale cultivation using low-cost substrates Long-term reagent performance under continuous operation. These findings will further advance research into the stability of *Rhodotorula rubra* in complex pulp systems and the cost-effectiveness of large-scale cultures, advancing the sustainable mineral processing paradigm.

Acknowledgments

Financial assistance was supported by the Central Guidance of Local Science and Technology Development Funds (Guike ZY24212034) and the National Natural Science Foundation of China (51464006).

References

ANGADI, S.I., SREENIVAS, T., JEON, H.-S., BAEK, S.-H., MISHRA, B.K. 2015. *A review of cassiterite beneficiation fundamentals and plant practices*. Miner Eng, 70, 178 - 200.

BALASUBRAMANIAN, V., HONNAVAR, R., SANKARAN, S., HEIDAR-ALI, T.R. 2012. *A novel property of DNA - as a bioflootation reagent in mineral processing*. PLoS One, 7(7), e39316.

CAO, A., WANG, Y., HUANG, J., LI, D., YANG, C. 2022. *Simulation Analysis on Drainage Mechanism of White Steel Mesh Under Fine Tailings*. Mod Min, 38(10), 190 - 192.

CHANG, Z., LI, Y., SHEN, Z., ZOU, L., WANG, Q., SUN, Z., WANG, H. 2023. *Advancements in the application and mechanism of fine - grained mineral flotation collectors*. Chin J Eng, 45(11), 1807 - 1819.

CHEN, M. 2009. *Study on effects of microorganisms on surface properties of chalcopyrite and adsorption mechanism* [master's thesis]. Changsha: Central South University.

CHEN, Y.-S. 2014. *Geological features and S isotope composition of tin deposit in Dachang ore district in Guangxi*. Trans Nonferr Met Soc China, 24(9), 2938 - 2945.

CHEN, Y., LI, H., FENG, D., TONG, X., HU, S., YANG, F., WANG, G. 2021. *A recipe of surfactant for the flotation of fine cassiterite particles*. Miner Eng, 160, 106658.

FU, L., LI, W., PAN, Z., ZHANG, Z., JIAO, F., QIN, W. 2024. *Synthesis of modified polystyrene nanoparticles and their application in fine cassiterite flotation*. Colloids Surf A. Physicochem Eng Asp, 681, 132608.

GONG, W., HE, J., YANG, B., XU, H., SHAN, Y., FU, L., WU, J., 2025. *Interfacial synergistic mechanism of an effective combined collector sodium oleate/cetyltrimethyl ammonium chloride and its enhanced flotation separation of K-feldspar and quartz*. Surfaces and Interfaces, 60, 106017.

GB/T 10574.1 - 2003. *Method for chemical analysis of tin - lead solder – Determination of tin content*. Beijing: General Administration of Quality Supervision, Inspection and Quarantine of the People's Republic of China.

GUO, W., ZHU, Y., WANG, P., LI, W., HAN, Y., LI, Y. 2016. *Experimental study on a new amide - carboxylic acid collector DWD - 1 used in reverse flotation of iron*. Miner Prot Util (China), (3), 22 - 25.

HEMALATHA, S., KANNAN, A.N. 2011. *Microbially induced flotation of alumina, silica/calcite from haematite*. Int J Miner Process, 99(1-4), 70 - 77.

JIANG, L., ZHOU, H., PENG, X. 2007. *Bio - oxidation of pyrite, chalcopyrite and pyrrhotite by Acidithiobacillus ferrooxidans*. Chin Sci Bull, 52(19), 2702 - 2714.

JIA, C.Y., WEI, D.Z., LI, P.J., LI, X.J., TAI, P.D., LIU, W., GONG, Z.Q. 2011. *Selective adsorption of Mycobacterium Phlei on pyrite and sphalerite*. Colloids Surf B Biointerfaces, 83(2), 214 - 219.

KORNELI, C., DAVID, F., BIEDENDIECK, R., JAHN, D., WITTMANN, C. 2013. *Getting the big beast to work: systems biotechnology of Bacillus megaterium for novel high - value proteins*. J Biotechnol, 163(2), 87 - 96.

LAN, L., YANG, Z., LAN, P., AI, G. 2015. *Progress of microorganisms in the field of mineral flotation separation*. Popul Sci Technol (China), 17(185): 61 - 65.

LI, D., YIN, W., MA, Y., YAO, J. 2016. *Effects of particle size distribution on hematite flotation*. J Northeast Univ (China), 37(6), 865 - 868.

LI, H.-D., YANG, C.-R., TIAN, Z.-Y., WU, C.-F., QIN, W.-Q. 2023. *Cassiterite beneficiation in China: a mini-review*. J Cent South Univ, 30(1), 1 - 19.

LIU, Y., DONG, Y., LIN, H., CHEN, Y., YU, M. 2014. *Pollution characteristics of heavy metals in typical tin mineral processing plant of Yunnan, China*. Chin J Nonferrous Met, 24(4), 1084 - 1090.

MERMA, A.G., TOREM, M.L., MORÁN, J.J.V., MONTE, M.B.M. 2013. *On the fundamental aspects of apatite and quartz flotation using a Gram positive strain as a bioreagent*. Miner Eng, 48: 61 - 67.

MIAO, Y., FENG, Q., WEN, S. 2024. *Experimental and MD study on the effect of SDS/OHA mixed collector coadsorption on cassiterite flotation*. Sep Purif Technol, 339, 126635.

PENG, R., WEI, Z., ZENG, M., WANG, H. 2019. *Research development of cassiterite collector*. Conserv Util Miner Resour (China), 39(4), 165 - 171.

QIU, L., ZHANG, X., ZHAO, Z., ZHOU, X. 2018. *Study on comprehensive utilization of multi - metal from the tin mine tailings with a combined separation method*. Nonferr Met Miner Process Sect, (4), 37 - 45.

QIU, Y., HUANG, Y. 2016. *Experimental study on combined separation of gravity and floatation on a low-grade refractory tin sludge from Yunnan Tin Corporation*. Nonferrous Met (China), (1), 31-35.

SARVAMANGALA, H., NATARAJAN, K.A. 2009. *Microbially induced flotation of galena and quartz from pyrite*. Adv Mater Res, 835(71-73), 509 - 512.

SHANG, Y. 2015. *Research on flotation of low-grade tungsten-tin from a certain multi-metal ore*. Min Eng, 13(5), 19 - 22.

SREENIVAS, T., PADMANABHAN, N.P.H. 2002. *Surface chemistry and flotation of cassiterite with alkyl hydroxamates*. Colloids Surf A Physicochem Eng Asp, 205(1-2), 47 - 59.

SU, Z., ZHANG, Y., LIU, B., LU, M., LI, G., JIANG, T. 2017. *Extraction and separation of tin from tin - bearing secondary resources: a review*. JOM, 69(11), 2364 - 2372.

VASANTHAKUMAR, B., RAVISHANKAR, H., SUBRAMANIAN, S. 2014. *Basic studies on the role of components of Bacillus megaterium as flotation biocollectors in sulphide mineral separation*. Appl Microbiol Biotechnol, 98(6), 2719 - 2728.

WANG, P. 2013. *Action of hydroxamic acids on minerals in the flotation of fine cassiterite [master' thesis]*. Changsha: Central South University.

WANG, T. 2015. *Recovery of low-grade fine cassiterite with a combined flowsheet of gravity separation-flotation-gravity separation*. Min Metall Eng (China), 35(6), 68 - 71.

XU, X., YU, Y., XU, X. 2013. *Separation behavior and mechanism of hematite and collophane in the presence of collector RFP-138*. Trans Nonferr Met Soc China, 23(2), 501 - 507.

YANG, B., HE, J., 2025. *New insights into selective depression mechanism of Tamarindus indicakernel gum in flotation separation of fluorapatite and calcite*. Separation and Purification Technology, 354(Part 3), 128787.

YANG, F., YANG, H., LIU, H., SUN, W. 2012. *Flotation separation of scheelite and calcite at ambient temperature using new quaternary ammonium salt as collector*. Trans Nonferr Met Soc China, 22(5), 200 - 206.

YANG, Z., LAN, L., AI, G., LAN, P., LIAO, A. 2016. *The Study of Selective Adsorption of Rhodotorula Rubra on Cassiterite and Quartz*. Sci Tech Eng, 16(19), 164 - 169.

YU, K.-P., YU, Y.-F., XU, X.-Y. 2013. *Separation behavior and mechanism of hematite and collophane in the presence of collector RFP-138*. Trans Nonferr Met Soc China, 23(2), 501 - 507.

YU, S., DUAN, H., CHEN, J. 2021. *An evaluation of the supply risk for China's strategic metallic mineral resources*. Resour Policy, 70, 101891.

YU, X. 2013. *Application of microbial technology in coal and gas desulfurization [master' thesis]*. Liaoning: University of Science and Technology Liaoning.

YIN, W.-Z., WANG, J.-Z. 2014. *Effects of particle size and particle interactions on scheelite flotation*. Trans Nonferr Met Soc China, 24(11), 3682 - 3687.

YUAN, X., YUAN, C., ZHONG, K., WEI, Y. 2000. *Study on microbiological processing technology of non-metallic mineral (I) – Thiobacillus ferrooxidans and its growth law*. China Nonmet Miner Ind Guide (China), (3), 12 - 14+23.

YUAN, X., YUAN, C., ZHONG, K., WEI, Y. 2000. *Study on microbiological processing technology of non-metallic minerals (II) – Study on microbiological flotation of pyrite*. China Nonmet Miner Ind Guide (China), (4), 17 - 19+24.

ZHANG, H. 2010. *Study on the mechanisms and application of combined collectors in fine cassiterite flotation [master' thesis]*. Changsha: Central South University; 89p.

ZHANG, L., KHOSO, S.A., TIAN, M., SUN, W. 2020. *Cassiterite recovery from a sulfide ore flotation tailing by combined gravity and flotation separations*. Physicochem Probl Miner Process, 57, 131006.

ZHANG, Y., LIU, D., LI, J., CAI, J., SHEN, P., CHEN, H. 2021. *A review on mechanism of flotation collector for cassiterite*. Chin J Nonferrous Met, 31(3), 785 - 795.

ZHU, L., LIU, J., GUO, Z., LV, L. 2020. *Effect and mechanism of oxalic acid on the floatability of cassiterite*. Metal Mine (China), (4), 72-77.

REN, L., ZHANG, Z., ZENG, W., ZHANG, Y., 2023. *Adhesion between nanobubbles and fine cassiterite particles*. International Journal of Mining Science and Technology, 33(4), 503-509.